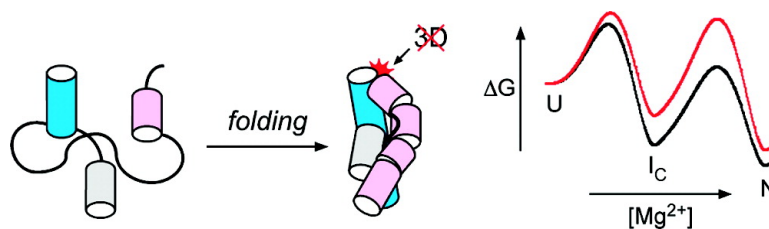


Tertiary Interactions Determine the Accuracy of RNA Folding

Seema Chauhan, and Sarah A. Woodson

J. Am. Chem. Soc., **2008**, 130 (4), 1296-1303 • DOI: 10.1021/ja076166i

Downloaded from <http://pubs.acs.org> on February 8, 2009



More About This Article

Additional resources and features associated with this article are available within the HTML version:

- Supporting Information
- Access to high resolution figures
- Links to articles and content related to this article
- Copyright permission to reproduce figures and/or text from this article

[View the Full Text HTML](#)

Tertiary Interactions Determine the Accuracy of RNA Folding

Seema Chauhan[†] and Sarah A. Woodson^{*‡}*Department of Chemistry and T.C. Jenkins Department of Biophysics, Johns Hopkins University, 3400 North Charles Street, Baltimore, Maryland 21218*

Received August 15, 2007; E-mail: swoodson@jhu.edu

Abstract: RNAs must fold into unique three-dimensional structures to function in the cell, but how each polynucleotide finds its native structure is not understood. To investigate whether the stability of the tertiary structure determines the speed and accuracy of RNA folding, docking of a tetraloop with its receptor in a bacterial group I ribozyme was perturbed by site-directed mutagenesis. Disruption of the tetraloop or its receptor destabilizes tertiary interactions throughout the ribozyme by 2–3 kcal/mol, demonstrating that tertiary interactions form cooperatively in the transition from a native-like intermediate to the native state. Nondenaturing PAGE and RNase T1 digestion showed that base pairs form less homogeneously in the mutant RNAs during the transition from the unfolded state to the intermediate. Thus, tertiary interactions between helices bias the ensemble of secondary structures toward native-like conformations. Time-resolved hydroxyl radical footprinting showed that the wild-type ribozyme folds completely within 5–20 ms. By contrast, only 40–60% of a tetraloop mutant ribozyme folds in 30–40 ms, with the remainder folding in 30–200 s via nonnative intermediates. Therefore, destabilization of tetraloop–receptor docking introduces an alternate folding pathway in the otherwise smooth energy landscape of the wild-type ribozyme. Our results show that stable tertiary structure increases the flux through folding pathways that lead directly and rapidly to the native structure.

Introduction

The self-assembly of biological macromolecules into a unique three-dimensional structure relies on the cooperation of many weak interactions. The cooperativity of these interactions determines the folding free energy landscape and the trajectory of the folding reaction.^{1,2} RNA folding landscapes are often rough, because RNA secondary structures are stable and form independently of weaker tertiary interactions.^{3,4} Consequently, RNA molecules frequently become trapped in metastable, misfolded structures in vitro.^{5,6} Understanding how RNAs avoid misfolding is crucial, because incorrectly folded RNAs may aggregate or be prematurely degraded in the cell. In this contribution, we report that the cooperativity of folding and the avoidance of misfolded intermediates in a bacterial ribozyme depend on the stability of the tertiary structure, rather than the base pairing potential.

The stabilities of RNA double helices can be predicted from empirical free energy parameters that account for the cooperativity of neighboring base pairs.⁷ By contrast, less is known about the thermodynamics of RNA tertiary interactions and

whether they cooperatively stabilize the native structure. In one study, adjacent hydrogen bonds in a “ribose zipper” motif added noncooperatively to the stability of the P4–P6 domain of *Tetrahymena* ribozyme.⁸ However, hydrogen bonds in small loops and pseudoknots form cooperative networks.⁹ Similarly, urea denaturation experiments suggested that at least three interdomain tertiary contacts in *Tetrahymena* ribozyme are energetically coupled to one another.¹⁰

In this study we examine the tertiary folding of a 195-nucleotide ribozyme derived from a self-splicing group I intron in *Azoarcus* pre-tRNA^{Ile}.¹¹ The *Azoarcus* ribozyme folds hierarchically, in that the core helices assemble in ~0.2 mM Mg²⁺, while stable tertiary structure and catalytic activity appear in ~2 mM Mg²⁺.^{12,13} Helix assembly correlates with global compaction of the RNA from the unfolded state (U; $R_g = 65 \pm 3 \text{ \AA}$) to an ensemble of compact intermediates (I_C; $R_g = 30.9 \pm 0.5 \text{ \AA}$) which have dimensions similar to those of the native state (N).^{13,14}

There are several indications that the I_C intermediate has a nativelike topology and contains some tertiary structure. First,

[†] Department of Chemistry.[‡] T.C. Jenkins Department of Biophysics.(1) Dill, K. A. *Protein Sci.* **1999**, *8*, 1166.(2) Thirumalai, D.; Hyeon, C. *Biochemistry* **2005**, *44*, 4957.(3) Brion, P.; Westhof, E. *Annu. Rev. Biophys. Biomol. Struct.* **1997**, *26*, 113.(4) Tinoco, I. J.; Bustamante, C. *J. Mol. Biol.* **1999**, *293*, 271.(5) Thirumalai, D.; Woodson, S. A. *Acc. Chem. Res.* **1996**, *29*, 433.(6) Treiber, D. K.; Williamson, J. R. *Curr. Opin. Struct. Biol.* **1999**, *9*, 339.(7) (a) Freier, S. M.; Kierzek, R.; Jaeger, J. A.; Sugimoto, N.; Caruthers, M. H.; Neilson, T.; Turner, D. H. *Proc. Natl. Acad. Sci. U.S.A.* **1986**, *83*, 9373.(b) Mathews, D. H.; Sabina, J.; Zuker, M.; Turner, D. H. *J. Mol. Biol.* **1999**, *288*, 911. (c) Siegfried, N. A.; Metzger, S. L.; Bevilacqua, P. C.*Biochemistry* **2007**, *46*, 172.(8) Silverman, S. K.; Cech, T. R. *Biochemistry* **1999**, *38*, 8691.(9) (a) Nixon, P. L.; Cornish, P. V.; Suram, S. V.; Giedroc, D. P. *Biochemistry* **2002**, *41*, 10665. (b) Moody, E. M.; Bevilacqua, P. C. *J. Am. Chem. Soc.* **2003**, *125*, 16285.(10) Ralston, C. Y.; He, Q.; Brenowitz, M.; Chance, M. R. *Nat. Struct. Biol.* **2000**, *7*, 371.(11) Reinhold-Hurek, B.; Shub, D. A. *Nature* **1992**, *357*, 173.(12) Rangan, P.; Masquida, B.; Westhof, E.; Woodson, S. A. *Proc. Natl. Acad. Sci. U.S.A.* **2003**, *100*, 1574.(13) Perez-Salas, U. A.; Rangan, P.; Krueger, S.; Briber, R. M.; Thirumalai, D.; Woodson, S. A. *Biochemistry* **2004**, *43*, 1746.(14) Chauhan, S.; Caliskan, G.; Briber, R. M.; Perez-Salas, U.; Rangan, P.; Thirumalai, D.; Woodson, S. A. *J. Mol. Biol.* **2005**, *353*, 1199.

R_g does not decrease significantly from I_C to N .¹³ Second, small-angle X-ray scattering studies showed that tertiary interactions between helices help stabilize I_C , even though the RNA backbone is accessible to bulk solvent in I_C .¹⁴ Third, unlike many multidomain RNAs, 80–90% of the *Azoarcus* ribozyme folds in less than 50 ms in 15 mM $MgCl_2$.¹² The rapid and concerted formation of the native tertiary structure suggests most of the *Azoarcus* ribozyme folds through natively intermediates, without becoming kinetically trapped in metastable structures.

To investigate the cooperativity of tertiary interactions in the *Azoarcus* ribozyme, we used site-directed mutagenesis to perturb a tetraloop–receptor interaction that bridges two major helical domains. We previously found that a mutation in the GAAA tetraloop of P9 (A190 to U), which disrupts docking with its receptor in J5/5a, globally destabilizes both the intermediate (I_C) and native states in *Azoarcus* ribozyme.¹⁴ Here, we compare local tertiary folding transitions in the wild-type and mutant RNAs using hydroxyl radical footprinting, which reports the average solvent accessibility of ribose C4' and C5' atoms at individual nucleotides.

We find that the disruption of tetraloop–receptor docking affects the formation of all other tertiary contacts in the RNA, demonstrating that tertiary interactions between helical domains are cooperative. Time-resolved footprinting experiments revealed that the P9 tetraloop mutation decreases the rate of direct folding to the native state and increases the fraction of the RNA population that initially misfolds. Our results suggest that the cooperative tertiary interactions enable a rapid and concerted folding of *Azoarcus* ribozyme, illustrating the association between cooperativity and the directness of the folding process.

Materials and Methods

RNA Preparation and Site-Directed Mutagenesis. The L-9 *Azoarcus* ribozyme (195 nt) was transcribed from pAz-IVS DNA digested with *Ear* I as previously described.¹² The RNA was resuspended in TE buffer (10 mM Tris-HCl, pH 7.5, 0.1 mM EDTA) before use. P9 loop mutants were prepared by mutating nucleotides A190 to U (GUAA) and A191 to G (GUGA) by PCR amplification of pAz-IVS and subsequent cloning into pUC18. The J5/5a receptor mutant (RGUAA) was engineered by introducing mutations C60 to G, A64 to C, G65 to U, U80 to A, U82 to G, and G84 to C by inverse PCR amplification of pAz-IVS and cloning into pUC18. The compensatory double mutant, R'GUAA, was prepared by replacing A190 with U by direct PCR amplification of pAz-RGUAAIVS and subcloning into pUC18.

Nondenaturing Gel Electrophoresis. Refolding experiments were carried out in CE buffer (10 mM sodium cacodylate, pH 7.0, 0.1 mM EDTA), 10% (v/v) glycerol, 0.1% (w/v) xylene cyanol, and 0–50 mM $MgCl_2$ at 50 °C as previously described.¹² The fraction of native RNA, f_N , was determined from the ratio of counts in band N relative to total counts in the lane. The fraction of native RNA as a function of Mg^{2+} concentration was normalized to the extent of folding at saturation and fit to the Hill equation. The maximum extent of folding at 50 °C was typically 80%, presumably reflecting a small population that remained trapped in misfolded conformations.

RNase T1 Cleavage. Partial RNase T1 digestion was carried out in 10 mM Tris-HCl (pH 7.5) plus 0–20 mM $MgCl_2$ at 50 °C.^{12,14} Fractional saturation (\bar{Y}) of each protection was normalized to 100% observed at 20 mM Mg^{2+} , and the data were fit to the Hill equation.

Hydroxyl Radical Footprinting. Fe(II)-EDTA-dependent hydroxyl radical cleavage reactions were carried out as previously described,¹² except that 5'-³²P-labeled RNA (400,000 cpm) was incubated in CE buffer plus 0–50 mM $MgCl_2$ for 15 min at 50 °C and 5 min on ice,

before the addition of Fenton reagents. Samples were heated to 95 °C in a formamide dye before loading on an 8% (w/v) sequencing gel. Sequence markers were prepared using RNase T1 or by cleavage of transcripts containing one phosphorothioate analogue (AαS or GαS) in 10 mM I_2 -ethanol.¹⁵

The relative extent of protection (\bar{Y}) was determined by comparing the intensity of bands in protected regions with cleavage products whose intensity does not change with Mg^{2+} concentration to correct for variations in sample recovery and loading.¹⁶ Fractional saturation of each protection (\bar{Y}) versus $MgCl_2$ concentration was fit to the Hill equation. The apparent Mg^{2+} -dependent free energy associated with formation of each tertiary contact was calculated by linear extrapolation from the transition midpoint, $\Delta G_{prot} = -n_H RT \ln(C/C_m)$,^{17,18} in which n_H is the Hill coefficient, C_m is the midpoint of the transition, and C is the Mg^{2+} concentration. This analysis assumes that an individual backbone contact is either completely formed or completely open. The free energy perturbation in the mutant relative to wild type was calculated from $\Delta\Delta G_{prot} = \Delta G_{prot}^{WT} - \Delta G_{prot}^{mut}$.

Fast Fenton Footprinting. Time-resolved Fe(II)-EDTA-dependent hydroxyl radical cleavage reactions were carried out as described.¹⁹ Folding reactions were initiated by mixing 15 μ L of 5'-³²P-labeled RNA (800,000 cpm) in CE with an equal volume of CE + 15 mM $MgCl_2$ and 0.15% hydrogen peroxide using a Kintek RQF-3 three-syringe mixer, at 37 °C. After the desired folding delay, the samples were mixed with 1 mM Fe(II)-EDTA via the third quench syringe. The samples were immediately expelled (5–10 ms) into a 20 μ L quench solution containing 3.2 M NaCl, 25 mM EDTA 0.1 μ g/ μ L carrier tRNA, and 0.26 μ g/ μ L glycogen. Under these conditions, the majority of cleavage occurs within 1–2 ms of Fe(II)-EDTA addition.¹⁹ The cleaved products were precipitated with three volumes of ethanol at –20 °C and separated on an 8% (w/v) sequencing gel. The gels were analyzed and quantified as described above. The wild-type and mutant data were fit to the single and double exponential rate equations, which were $\bar{Y} = A(1 - \exp(-k_{obs}t))$ and $\bar{Y} = A_{fast}(1 - \exp(-k_{fast}t)) + A_{slow}(1 - \exp(-k_{slow}t))$, respectively.

Results

Perturbation of Tetraloop–Receptor Docking. GNRA tetraloops are common in RNA secondary structures,²⁰ and their interactions with helical receptors elsewhere in the RNA stabilize its 3D architecture.^{21,22} The *Azoarcus* ribozyme contains two GAAA tetraloops. The tetraloop of paired region P9 docks with an 11-nucleotide motif in joining region J5/5a, while the tetraloop at the end of P2 docks with J8/8a (Figure 1).^{23,24} These tetraloop–receptor interactions clamp together helices at the opposite ends of the catalytic core.

The stability of the P9–J5/5a tetraloop–receptor interaction was perturbed by combining different loop and receptor sequences that are known to have varying stability (Figure 1A).²⁵ The GAAA tetraloop in P9 was changed to GUAA and GUGA. Both GUAA and GUGA tetraloops conform to the GNRA

- (15) Ryder, S. P.; Ortoleva-Donnelly, L.; Kosek, A. B.; Strobel, S. A. *Methods Enzymol.* **2000**, *317*, 92.
- (16) Sclavi, B.; Woodson, S.; Sullivan, M.; Chance, M.; Brenowitz, M. *Methods Enzymol.* **1998**, *295*, 379.
- (17) Cantor, C. R.; Schimmel, P. R. *The Behavior of Biological Macromolecules*; W. H. Freeman: San Francisco, 1980; Vol. III, p 1371.
- (18) Fang, X.; Pan, T.; Sosnick, T. R. *Biochemistry* **1999**, *38*, 16840.
- (19) Shcherbakova, I.; Mitra, S.; Beer, R. H.; Brenowitz, M. *Nucleic Acids Res.* **2006**, *34*, e48.
- (20) Woese, C. R.; Winker, S.; Gutell, R. R. *Proc. Natl. Acad. Sci. U.S.A.* **1990**, *87*, 8467.
- (21) (a) Murphy, F. L.; Cech, T. R. *J. Mol. Biol.* **1994**, *236*, 49. (b) Costa, M.; Michel, F. *EMBO J.* **1995**, *14*, 1276.
- (22) Jaeger, L.; Michel, F.; Westhof, E. *J. Mol. Biol.* **1994**, *236*, 1271.
- (23) Tanner, M.; Cech, T. *RNA* **1996**, *2*, 74.
- (24) Ikawa, Y.; Naito, D.; Aono, N.; Shiraishi, H.; Inoue, T. *Nucleic Acids Res.* **1999**, *27*, 1859.
- (25) Jaeger, L.; Westhof, E.; Leontis, N. B. *Nucleic Acids Res.* **2001**, *29*, 455.

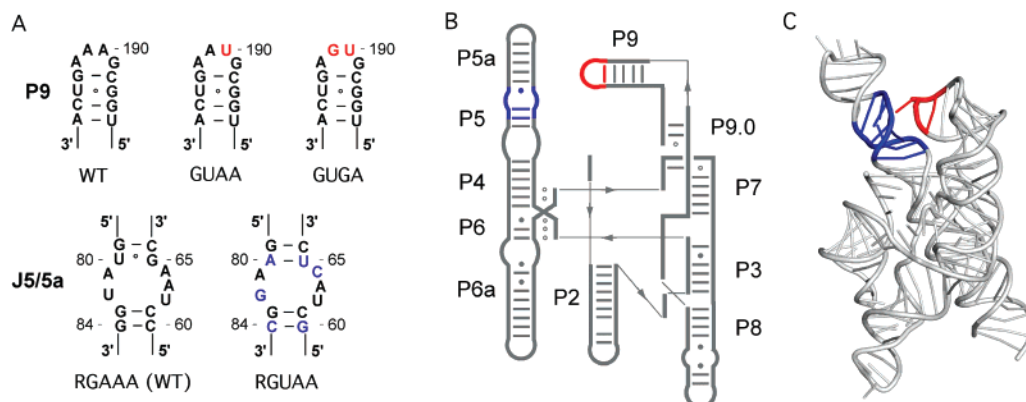


Figure 1. Mutagenesis of tertiary interactions in the *Azoarcus* ribozyme. (A) Sequence of P9 tetraloop and J5/5a 11-nt canonical receptor motif. Base substitutions are shown in red and blue, respectively. (B) Secondary structure of the L-9 ribozyme. P9-tetraloop, red; J5/5a-receptor, blue. (C) Ribbon diagram of the three-dimensional structure (PDB 1U6B⁶¹) colored as in B; created with Pymol (DeLano Scientific; <http://pymol.sourceforge.net>).

consensus sequence, but they preferentially interact with CC:GG and CU:AG tandem base pairs, respectively.^{22,26} The 11 nt receptor [CCUAAG...UAUGG] in J5/5a, which is specific for GAAA tetraloops, was replaced with the sequence [GC-UACU...AAGGC], which interacts strongly with GUAA tetraloops (RGUAA).²⁷ Finally, we made a compensatory double mutant, R'GUAA, that combines the GUAA tetraloop with the GUAA tetraloop receptor.

Mutants Destabilize the Compact State. To determine if the disruption of native tetraloop–receptor interactions introduces new nonnative intermediates, native and nonnative forms of wild-type and mutant RNAs were resolved by nondenaturing gel electrophoresis at 4–10 °C (Figure 2A). The native RNA (N) migrates more rapidly in the gel than the nonnative conformers (nn). Under these conditions, further refolding is arrested after the RNA enters the gel matrix.²⁸ Because the *Azoarcus* ribozyme folds rapidly, near-native intermediates (I_c) are also trapped in the native conformation and migrate at the same speed as the native RNA (N).¹² Thus, this method detects the U to I_c transition, which involves assembly of helices in the ribozyme core.

Uniformly radiolabeled wild-type and mutant ribozymes were incubated in increasing Mg²⁺ concentrations at 50 °C for 15 min and separated on a 10% native gel containing 3 mM MgCl₂. For the wild-type RNA, the midpoint of the folding transition (C_m) was 0.26 (±0.03) mM, which is similar to the midpoint of the collapse transition monitored by SAXS (0.34 mM Mg²⁺).¹⁴ All of the mutated RNAs required higher Mg²⁺ concentrations to fold correctly (C_m = 0.31–0.47 mM; Figure 2B). Even in 50 mM MgCl₂, only 40–50% of the mutant RNA was native, compared with ≥80% of the wild-type RNA. These results show that mutations in the tetraloop or in the receptor disfavor the formation of natively intermediates, consistent with previous biochemical and SAXS results on the GUAA mutant obtained under slightly different conditions.¹⁴ Although compensation of the tetraloop–receptor interaction was expected to restore the stability of the folded ribozyme,²⁷ the R'GUAA double mutant did not fold as well as the wild-type RNA.

Disruption of the interaction between P9 and J5/5a not only destabilized I_c but also increased the conformational heterogene-

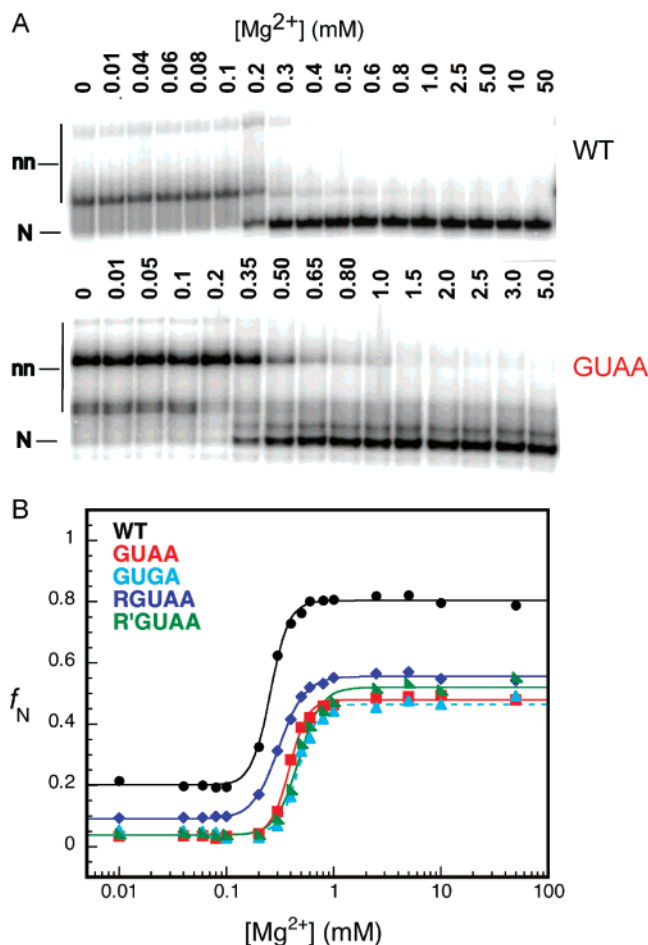


Figure 2. Folding of *Azoarcus* ribozyme by native PAGE. (A) WT, wild-type ribozyme; GUAA, P9 tetraloop mutation. Bands nn, nonnative folding intermediates; N, native RNA. Native PAGE for other mutants are shown in Figure S1. (B) Mg²⁺-dependence of folding. The fraction of native RNA was fit to the Hill equation (see Materials and Methods). Wild-type: (black ●) (C_m = 0.26 ± 0.01 mM, n_H = 4.9 ± 0.3); GUAA: (red ■) (C_m = 0.43 ± 0.01 mM, n_H = 3.9 ± 0.3); GUGA: (cyan ▲) (C_m = 0.47 ± 0.01 mM, n_H = 4.9 ± 0.5); RGUAA: (blue ◆) (C_m = 0.31 ± 0.01 mM, n_H = 3.6 ± 0.2), and R'GUAA: (green ▼) (C_m = 0.47 ± 0.01 mM, n_H = 4.1 ± 0.4).

ity of the RNA population. First, all of the mutated RNAs, except RGUAA, exhibited two distinct populations of nonnative intermediates (nn) (Figure S1). Second, the mutants migrated more slowly than the wild-type RNA in the folded and unfolded states, indicating that none of the mutants is as compact as the

(26) Pley, H. W.; Flaherty, K. M.; McKay, D. B. *Nature* **1994**, *372*, 111.

(27) Costa, M.; Michel, F. *EMBO J.* **1997**, *16*, 3289.

(28) Emerick, V. L.; Woodson, S. A. *Proc. Natl. Acad. Sci. U.S.A.* **1994**, *91*, 9675.

wild-type RNA (S.C., unpublished results). Finally, when the RNA was preincubated in buffer without Mg^{2+} , 20% of wild-type RNA folded to N during the 5–15 s that the sample encounters Mg^{2+} in the gel running buffer (4 °C). By contrast, only 5–10% of the mutant RNAs folded correctly in this time (Figure 2B). Thus, the wild-type RNA has a greater probability of forming native-like conformations in a short time than does the mutant RNA.

Secondary Structure and Helix Assembly. We previously found that native gel mobility and metal ion-induced collapse correlates with the assembly of helices in the catalytic core, which become base paired in submillimolar Mg^{2+} .^{12,13} To assess the effect of mutations on base pairing of core helices, the wild-type RNA, GUAA, and GUGA loop mutants were partially digested with RNase T1 in various Mg^{2+} concentrations. The cleavage patterns of all RNAs were similar to what we observed previously.¹² Guanosines in P2, P4, P5/5a, P6a, and P9 were protected from cleavage in 10 mM Tris-HCl alone (Figure S2). G's in P3, P6, P7, P8a, J8/7, and P9.0 were protected from RNase T1 with increasing Mg^{2+} , except G163–G166 in P8, which were first cleaved more strongly, then protected with $C_m = 0.45$ mM $MgCl_2$.

As expected, G's in the core of the GUAA and GUGA tetraloop mutants required more Mg^{2+} ($C_m = 0.1$ – 0.7 mM) to become base paired than the same residues in the wild type RNA ($C_m = 0.1$ – 0.3 mM) (Figures 3A and S3; Table S1). Moreover, protection of individual G's from RNase T1 increased less cooperatively with respect to Mg^{2+} concentration in the mutants, and the Mg^{2+} -dependence of forming individual base pairs varied more in the loop mutants compared with the wild-type RNA (Figure 3B). Thus, destabilization of I_C reduces the apparent cooperativity of helix assembly. This is unlikely to be due to direct perturbation of the RNA secondary structure by the base substitutions in P9, because G's far from P9 are as strongly affected as those nearby and because base substitutions in the J5/5a receptor and in J6/7 produce similar results (Figure S2;¹⁴). Instead, we conclude that tertiary interactions between helical domains help drive the ensemble of base paired conformations toward a narrower subset of native-like structures.

Cooperativity of Tertiary Folding. As mutations in the P9 tetraloop destabilize the native ribozyme, we next asked whether loss of this tetraloop–receptor interaction influences the formation of tertiary interactions elsewhere in the RNA. The stabilities of individual tertiary interactions were probed by Fe(II)-EDTA-dependent hydroxyl radical cleavage, which is sensitive to the solvent accessibility of the RNA backbone.²⁹ The average accessibility of the RNA backbone reflects the equilibrium between open and closed states for each chain segment. This equilibrium depends on local fluctuations that expose the RNA backbone to solvent and on global unfolding. This same principle is used in hydrogen/deuterium exchange studies of protein folding.³⁰

If folding were perfectly cooperative (the RNA is either completely unfolded or completely folded), we expect residues in different parts of the RNA to become protected at the same Mg^{2+} concentration. If the tertiary interactions form independently of one another, we expect residues in different parts of

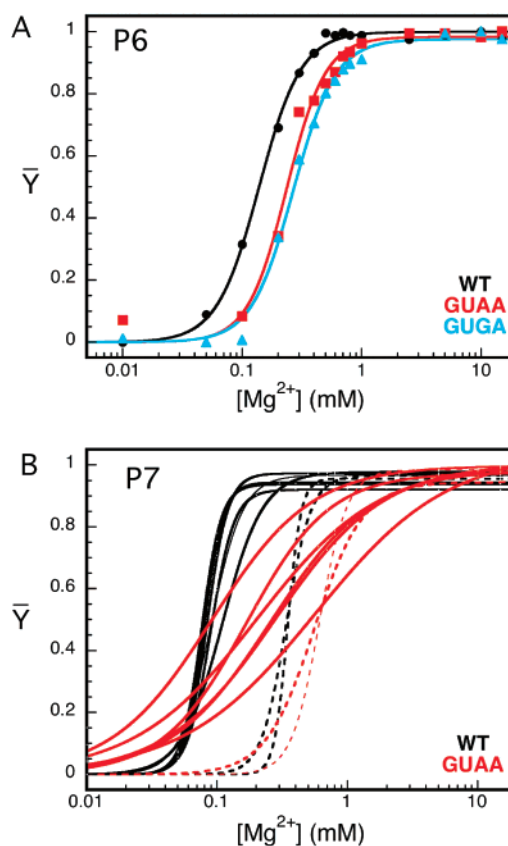


Figure 3. Helix assembly in the *Azoarcus* ribozyme. Formation of core helices was monitored by partial digestion with RNase T1. (A) Mg^{2+} -dependence of RNase T1 protection in P6 (nt 122–126). Wild-type: (black ●) ($C_m = 0.14 \pm 0.01$ mM, $n_H = 2.5 \pm 0.11$); GUAA: (red ■) ($C_m = 0.23 \pm 0.02$ mM, $n_H = 2.7 \pm 0.3$); GUGA: (cyan ▲) ($C_m = 0.27 \pm 0.01$ mM, $n_H = 2.5 \pm 0.2$). (B) Fractional saturation of RNase T1 protection at G's throughout the secondary structure (fitted curves only). Wild-type (black) and GUAA (red). Dashed lines represent nt in P3 and P8. Data for individual positions are shown in Figure S3 and Table S1.

the RNA to become protected at different Mg^{2+} concentrations. This is because individual tertiary contacts, which typically involve different types of noncovalent interactions, will have different free energies of formation and will depend differently on the bulk Mg^{2+} concentration.^{10,31}

The hydroxyl radical cleavage patterns for the wild-type and mutant ribozymes were similar to each other and to those from our previous results on the wild-type RNA.¹² Residues that are buried in the tertiary structure were increasingly protected from cleavage as the Mg^{2+} concentration was raised to 15 mM (see Figure S5 for details), and the extent of backbone protection correlated with the increase in catalytic activity. In the wild-type ribozyme, the midpoints for individual protected regions overlap within the experimental error ($C_m = 1$ mM $MgCl_2$, $n_H = 2$; Figure 4a and Table 1), except for residues in P4, the J5/5a receptor and J4/5, which require slightly more Mg^{2+} to be protected ($C_m = 1.8$ mM). Nucleotides in P4 and J4/5 dock the P1 splice site helix,³² and their interactions may be compromised in our exon-less ribozyme. The formation of most tertiary contacts over a narrow range of Mg^{2+} concentration is

(29) Tullius, T. D.; Greenbaum, J. A. *Curr. Opin. Chem. Biol.* **2005**, *9*, 127.
 (30) (a) Englander, S. W.; Mayne, L.; Bai, Y.; Sosnick, T. R. *Protein Sci.* **1997**, *6*, 1101. (b) Chamberlain, A. K.; Marqusee, S. *Structure* **1997**, *5*, 859.

(31) Pan, J.; Thirumalai, D.; Woodson, S. A. *Proc. Natl. Acad. Sci. U.S.A.* **1999**, *96*, 6149.
 (32) (a) Wang, J. F.; Cech, T. R. *Science* **1992**, *256*, 526. (b) Strobel, S. A.; Cech, T. R. *Science* **1995**, *267*, 675.

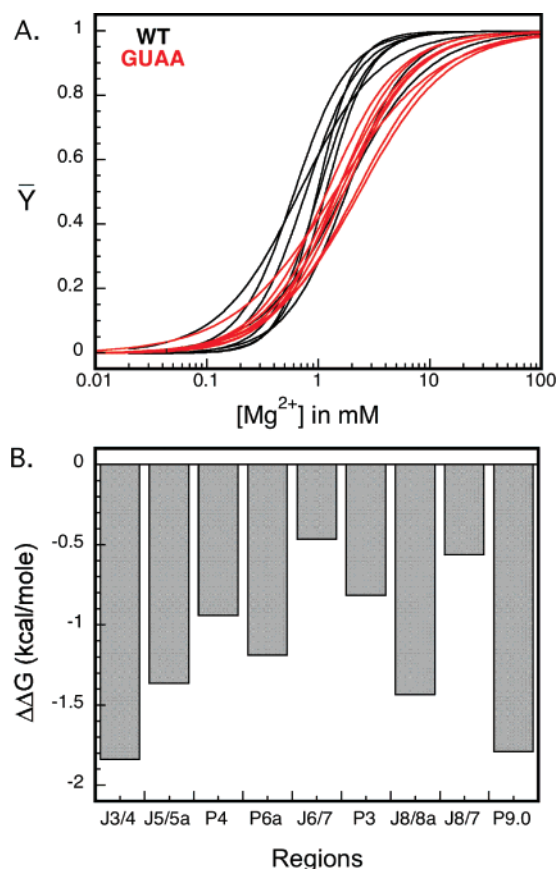


Figure 4. Mg^{2+} -dependence of tertiary contacts. Solvent accessibility of the RNA backbone was probed by Fe(II)-dependent hydroxyl radical cleavage. (A) Fractional saturation of protections from hydroxyl radicals across all tertiary contacts in wild-type (black) and GUAA (red) ribozymes. Data for individual positions are shown in Figure S6. All data were fit to the Hill equation assuming a single open and closed state for each residue. (B) Free energy of forming individual backbone contacts ($\Delta\Delta G_{\text{prot}}$) in the wild-type ribozyme relative to the GUAA ribozyme in 15 mM $MgCl_2$ (see Materials and Methods).

Table 1. Mg^{2+} -Dependence of RNA Backbone Contacts^a

regions	nts	WT		GUAA	
		C_m (mM)	n_H	C_m (mM)	n_H
J3/4	49–50	1.1 ± 0.2	2.4 ± 0.6	1.20 ± 0.07	1.3 ± 0.1
J5/5a	62–64	1.8 ± 0.2	2.0 ± 0.3	2.5 ± 0.1	1.2 ± 0.1
J4/5, P4	86–89	1.7 ± 0.2	1.8 ± 0.7	2.15 ± 0.07	1.19 ± 0.07
J6/6a, P6a	96–101	1.5 ± 0.4	2.2 ± 0.8	1.5 ± 0.3	1.4 ± 0.4
P6, J6/7, P7	123–130	1.3 ± 0.2	1.5 ± 0.3	1.4 ± 0.5	1.3 ± 0.1
P3	137–142	0.8 ± 0.2	1.5 ± 0.3	1.6 ± 0.2	1.3 ± 0.2
J8/8a	148–151	0.66 ± 0.03	1.4 ± 0.3	1.4 ± 0.1	0.90 ± 0.07
J8/7	165–172	0.8 ± 0.2	1.2 ± 0.2	1.6 ± 0.6	1.16 ± 0.09
P9.0	180–182	0.69 ± 0.03	1.9 ± 1.5	1.0 ± 0.4	1.1 ± 1.0

^a The formation of tertiary interactions at 50 °C was monitored by hydroxyl radical cleavage in the wild-type and loop mutant, GUAA. Data from three independent trials were fit to the Hill equation as shown in Figure 4a and Figure S5. Reported are the mean and standard deviation of midpoints (C_m) and Hill coefficients (n_H) between these trials.

consistent with a cooperative transition from I_C to N in the wild-type ribozyme.

Energetic Coupling between Tertiary Contacts. Hydroxyl radical footprinting experiments showed that all of the tertiary contacts in the GUAA ribozyme appear at higher Mg^{2+} concentrations ($C_m = 0.9$ to 2.5 mM; $n_H = 1$) than the same contacts in the wild-type ribozyme (Figures 4a and S6; Table 1). Other tetraloop and receptor mutations caused similar

increases in the midpoints of the folding transitions (data not shown). Thus, disruption of the interaction between the P9 tetraloop and its receptor in J5/5a at one end of the ribozyme causes nearly equal destabilization of tertiary contacts elsewhere in the RNA. In addition, the GUAA mutation causes individual tertiary contacts to saturate over a broader range of Mg^{2+} concentration, suggesting an increased presence of folding intermediates.

Since the cooperativity and the midpoint of Mg^{2+} -induced folding are related to the free energy gap between the unfolded and folded states,^{18,31} we obtained the free energy of forming individual tertiary contacts from the Mg^{2+} dependence of each hydroxyl radical protection (see Materials and Methods). In the wild-type ribozyme, the free energies for forming individual tertiary contacts (ΔG_{prot}) ranged from -2.2 to -4.0 kcal/mol, whereas the GUAA tetraloop mutation made all of the tertiary contacts in the ribozyme less favorable, with free energies ranging from -1.4 to -2.2 kcal/mol (Figure 4b). The largest perturbations to ΔG_{prot} were observed in the J5/5a receptor, in J3/4 that base triples with P6, in J8/8a that docks the P2 tetraloop, and in P9.0 that forms a reverse kink turn with P9.³³ This global destabilization of tertiary structure is a hallmark of cooperative structures.

The thermodynamic destabilization at individual residues (1.4–2.2 kcal/mol) measured by hydroxyl radical footprinting is comparable to the global destabilization of the native state (1.2 kcal/mol) estimated from the Mg^{2+} dependence of catalytic activity.¹⁴ The *Tetrahymena* ribozyme and its P4–P6 domain are also destabilized by 2–4 kcal/mol upon disruption of peripheral tetraloop–receptor interactions.^{10,34,35}

Rapid Folding of the Wild-Type Ribozyme. The results above show that the U to I_C and I_C to N folding transitions become less cooperative when the RNA tertiary structure is destabilized. To determine whether this apparent loss of cooperativity also reduces the specificity of the folding pathways, we probed the folding kinetics of the *Azoarcus* ribozyme by time-resolved hydroxyl radical footprinting. By delivering the Fe(II)-EDTA with a rapid quench apparatus, changes in the RNA tertiary structure can be detected within 2–5 ms.¹⁹ This method was previously used to resolve folding intermediates of the *Tetrahymena* ribozyme.³⁶

The folding kinetics of the *Azoarcus* ribozyme was measured by quantifying the changes in solvent accessibility of individual sites as a function of time (Figure S7). After addition of 15 mM Mg^{2+} at 37 °C, all of the nucleotides that are buried in the folded RNA were 80–100% protected from hydroxyl radical cleavage within 10 ms (Figure 5 and Figure S8). These results corroborate our earlier observation using X-ray footprinting that the *Azoarcus* ribozyme folds rapidly without becoming trapped in metastable intermediates.¹² The better time resolution of the rapid quench method, however, shortens our estimate of the folding time from 30–50 ms to 5–20 ms ($k \approx 50$ –150 s^{-1} ; Table S2). This is comparable to the folding times reported for

(33) Strobel, S. A.; Adams, P. L.; Stahley, M. R.; Wang, J. *RNA* **2004**, *10*, 1852.

(34) Treiber, D. K.; Williamson, J. R. *J. Mol. Biol.* **2001**, *305*, 11.

(35) Young, B. T.; Silverman, S. K. *Biochemistry* **2002**, *41*, 12271.

(36) Laederach, A.; Shcherbakova, I.; Liang, M. P.; Brenowitz, M.; Altman, R. B. *J. Mol. Biol.* **2006**, *358*, 1179.

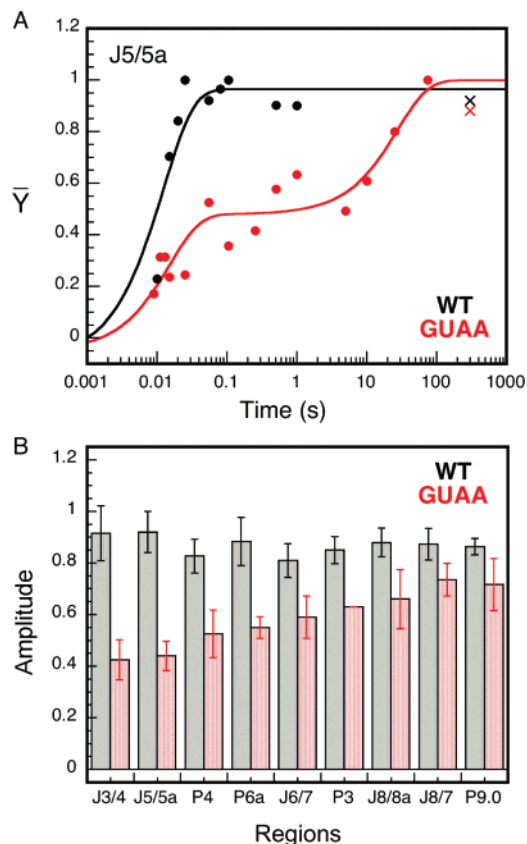


Figure 5. Tertiary folding kinetics of the *Azoarcus* ribozyme. (A) Fractional saturation of protection in P5/5a (nt 62–63) from time-resolved Fe(II)-EDTA hydroxyl radical cleavage. Wild-type: (●) ($k = 96 \pm 20 \text{ s}^{-1}$, $A = 0.97 \pm 0.06$); GUAA: (○) ($k_{\text{fast}} = 56 \pm 16 \text{ s}^{-1}$, $A_{\text{fast}} = 0.48 \pm 0.04$; $k_{\text{slow}} = 0.04 \pm 0.02 \text{ s}^{-1}$, $A_{\text{slow}} = 0.52 \pm 0.01$). Data were fit to single or double exponential rate equations. (×) RNA pre-folded in 15 mM MgCl₂. The data for other positions are presented in Figure S8 and Table S2. B. Amplitude of the burst phase across all tertiary contacts in the ribozyme. Wild-type, shaded bars; GUAA, open bars.

tRNA (10 ms)³⁷ and the 160 nt P4–P6 RNA (35–350 ms)^{38,39} and is much shorter than the typical folding time of large ribozymes.⁴⁰ The rapid folding kinetics in the *Azoarcus* ribozyme is probably the outcome of a metal ion-induced collapse that specifically leads to native-like intermediates.

Mutations Reveal a Rugged Folding Landscape. To determine if destabilization of tertiary interactions introduces new folding intermediates, the folding kinetics of the wild-type and GUAA ribozymes were compared (Figures 5 and S7). In contrast to the wild-type RNA, which folds in a single kinetic phase over the accessible time window, tertiary contacts in the GUAA ribozyme formed in two kinetic phases (Figures 5A and S8). Although 40–70% of the RNA folded in the first 20 ms ($k_{\text{fast}} \approx 50 \text{ s}^{-1}$), the remaining 30–60% of each backbone protection saturated over 30–200 s ($k_{\text{slow}} \approx 0.005\text{--}0.03 \text{ s}^{-1}$; Table S2). Thus, the GUAA mutation slightly decreases the initial folding rate and reduces the fraction of the RNA

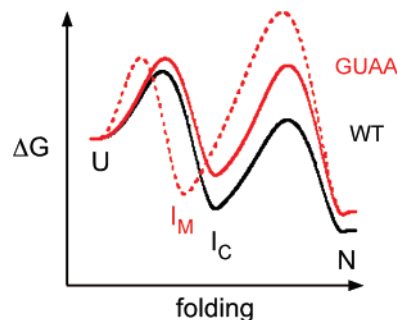


Figure 6. Free energy landscape for folding the *Azoarcus* ribozyme. The wild-type ribozyme (black) folds to N with $\tau_{\text{obs}} \approx 5 \text{ ms}$ via the native-like intermediate I_C. The GUAA ribozyme (red) folds along at least two pathways, via I_C or a metastable intermediate I_M ($\tau_{\text{obs}} \approx 40 \text{ ms}$ and 100 s). Free energies of I_C and N relative to U were taken from the Mg²⁺-dependence of native PAGE (ΔG_{UI}) and ribozyme activity (ΔG_{IN}) at 50 °C in 1 and 5 mM MgCl₂, respectively.¹⁴ The energy barriers were scaled in proportion to the folding times (τ_{obs}) at 37 °C, assuming $\tau_{\text{obs}} = \tau_0 e^{\ddagger}$ and $\tau_0 \approx 1 \mu\text{s}$. The relative energy barriers are expected to scale similarly between 37° and 50 °C.

population that rapidly forms the native tertiary structure. The small decrease in the initial folding rate may reflect the destabilization of N. After the initial burst, tertiary contacts in J8/8a and J8/7 form 10,000-fold more slowly in the GUAA ribozyme than in the wild-type ribozyme.

These results demonstrate that destabilization of the tetraloop–receptor interaction allows new folding pathways to become populated (Figure 6). Loss of a tertiary contact introduces ruggedness in the otherwise smooth folding landscape of the wild-type *Azoarcus* ribozyme. The more rugged energy landscape of the mutant RNA likely results from thermodynamic destabilization of a native-like, on-path compact intermediate,¹⁴ which decreases the specificity of the initial collapse transition in the mutant RNAs. Initial stopped-flow fluorescence experiments show that other tertiary mutations in the *Azoarcus* ribozyme also increase the extent of misfolding (S.C. and S.W., unpublished). By contrast, similar mutations in the isolated P4–P6 domain and the entire *Tetrahymena* ribozyme had milder effects on the folding kinetics.^{34,35,38} This may reflect the propensity of those RNAs to fold via partially misfolded intermediates, so that the observed folding rate depends on structural rearrangements later in the folding process rather than on the specificity of the initial collapse.

Discussion

Our results on the *Azoarcus* ribozyme establish a correlation between cooperativity and accuracy in RNA folding that was suggested in earlier work on the *Tetrahymena* ribozyme.³¹ Because RNA structures are stabilized by many weak, noncovalent interactions, the stability of the folded RNA increases with the number of energetically favorable interactions that are present in the native state but not in the unfolded RNA. Theoretical models and experiments show that the cooperativity, stability, and folding kinetics all depend on the degree to which the interactions uniquely specify the three-dimensional structure.^{3,41,42} As the interactions that stabilize the native state become more cooperative, intermediate structures are less populated, and the free energy gap between the native and unfolded states becomes larger.

Strong cooperativity among native interactions (and a low potential for topological frustration) produces a smooth free

(37) Cole, P. E.; Crothers, D. M. *Biochemistry* **1972**, *11*, 4368. (38) Deras, M. L.; Brenowitz, M.; Ralston, C. Y.; Chance, M. R.; Woodson, S. A. *Biochemistry* **2000**, *39*, 10975. (39) Silverman, S. K.; Deras, M. L.; Woodson, S. A.; Scaringe, S. A.; Cech, T. R. *Biochemistry* **2000**, *39*, 12465. (40) (a) Zarrinkar, P. P.; Williamson, J. R. *Science* **1994**, *265*, 918. (b) Fang, X. W.; Pan, T.; Sosnick, T. R. *Nat. Struct. Biol.* **1999**, *6*, 1091. (c) Swisher, J. F.; Su, L. J.; Brenowitz, M.; Anderson, V. E.; Pyle, A. M. *J. Mol. Biol.* **2002**, *315*, 297. (d) Xiao, M.; Leibowitz, M. J.; Zhang, Y. *Nucleic Acids Res.* **2003**, *31*, 3901.

energy landscape that allows most of the molecules to faithfully collapse toward the native state.² By contrast, low cooperativity among native interactions creates a rough free energy landscape and increases the probability that some molecules in the population become kinetically trapped in misfolded intermediates.⁵ Our results on the *Azoarcus* ribozyme show that tertiary interactions not only stabilize the I_C and N states but also contribute significantly to the accuracy and the speed of RNA folding.

The presence of tertiary interactions in I_C is unexpected, because backbone contacts are not directly detected by hydroxyl radical footprinting under conditions that populate I_C. However, the conclusion that tertiary interactions stabilize I_C is supported by thermal melting data and by SAXS experiments which measured the global collapse transition in the GUAA mutant and in ribozymes with mutations in P3 and the central triple helix.¹⁴ Studies on the P4–P6 RNA and the bI5 ribozyme also found evidence for native interactions in compact RNA intermediates.⁴³ One possibility is that the tertiary interactions in I_C are dynamic, allowing solvent (and hydroxyl radical) to enter the RNA interior.

Specificity of Helix Assembly. The extent of misfolding in RNA is usually attributed to the fact that a single sequence can form more than one stable secondary structure.⁴⁴ While the potential for mispairing is important, our results suggest that tertiary interactions restrict the number of base paired configurations that are allowed, significantly increasing the specificity of self-assembly. Mutations in P9 or J5/5a not only diminish the cooperativity of base pairing with respect to Mg²⁺ concentration, but also reduce the correlation between base pairs in different parts of the RNA.

There are several examples in which tertiary folding changes the secondary structure of the RNA, such as the alpha operon mRNA leader,⁴⁵ the P5abc subdomain of the *Tetrahymena* ribozyme,^{46a} and a stem-loop in the Varkud Satellite ribozyme.⁴⁷ Thus, although secondary structures are typically more stable than tertiary interactions in RNA, tertiary interactions can provide enough free energy to shift the equilibrium between different secondary structures.^{46b} Our results suggest that this is an important mechanism for prejudicing the ensemble of folding intermediates toward native-like structures.

In the *Azoarcus* ribozyme, the majority of base pairs in the core of the ribozyme form during the collapse transition from U to I_C, which requires counterions such as Mg²⁺. SAXS experiments showed that tertiary interactions, including docking of the P9 tetraloop with J5/5a, stabilize I_C.¹⁴ Because tertiary interactions often connect nucleotides that are far apart in the primary sequence, they constrain the global conformation of the RNA more powerfully than base pairs, which more often

join nearby residues. In the *Azoarcus* ribozyme, the cooperativity of tertiary interactions not only stabilizes the folded RNA but makes the collapse transition more specific.

Direct and Indirect Kinetic Folding Pathways. Because the initial collapse transition is specific and I_C contains mostly native-like structures, ≥80% of the wild type *Azoarcus* ribozyme folds within 5–20 ms in our experiments. By contrast, our time-resolved footprinting results show that disruption of native tertiary interactions between P9 and J5/5a in the mutants reduces the size of the fast folding population and increases the flux through alternative folding pathways (Figure 6). We also found that the initial folding transition appears slightly slower in the GUAA mutant than in the wild-type ribozyme. The observation that this mutation changes the partitioning between kinetic folding pathways supports the prediction that the smoothness of the folding landscape is directly related to the stability of the tertiary structure.

It is interesting to consider why some group I ribozymes fold rapidly, such as the *Azoarcus* ribozyme¹² and the ribozyme from *Candida* large subunit rRNA,⁴⁸ while others such as the *Tetrahymena* ribozyme tend to become trapped in misfolded intermediates.⁴⁹ In the *Tetrahymena* ribozyme, the native P3 helix is replaced by a stable alternative pairing (alt P3),⁵⁰ and the kinetic partitioning toward the direct (fast) folding pathway is sensitive to the relative stability of P3 and alt P3.⁵¹ Thus, the potential for mispairing contributes to the roughness of the free energy landscape.

Base pairing cannot be the only factor that determines the fidelity of the folding process, however, as the *Azoarcus* and *Candida* ribozymes can also mispair although they form less stable alternatives to P3 than the *Tetrahymena* ribozyme.⁴⁸ A critical difference, however, is that the P2 and P9 tetraloops can only dock with their receptors in the *Azoarcus* ribozyme when the core helices are correctly assembled. Thus, the formation of these and other tertiary interactions during the collapse transition preferentially stabilizes native helices relative to mispaired structures. By contrast, both correctly base paired and mispaired conformations of the *Tetrahymena* ribozyme are greatly stabilized by tertiary interactions between the peripheral P2, P2.1, P5c, and P9a helices.⁵² Mutations that destabilize these peripheral tertiary interactions accelerate folding, confirming that they help lock the *Tetrahymena* ribozyme in a misfolded state.^{34,53}

Cooperativity and Thermostability. The *Azoarcus* ribozyme is an unusually stable RNA, remaining active up to 75 °C or in 5 M urea.²³ This is surprising because the free energy changes associated with the formation of tertiary interactions in the I_C to N transition are only 2–3 kcal/mol in 10 mM MgCl₂ (Table 1). The thermostability of *Azoarcus* ribozyme, however, can

- (41) (a) Go, N. *Annu. Rev. Biophys. Bioeng.* **1983**, *12*, 183. (b) Creighton, T. E.; Darby, N. J.; Kemmink, J. *FASEB J.* **1996**, *10*, 110. (c) Onuchic, J. N.; Luthey-Schulten, Z.; Wolynes, P. G. *Annu. Rev. Phys. Chem.* **1997**, *48*, 545. (d) Luque, I.; Leavitt, S. A.; Freire, E. *Annu. Rev. Biophys. Biomol. Struct.* **2002**, *31*, 235. (e) Pyle, A. M.; Fedorova, O.; Waldsich, C. *Trends Biochem. Sci.* **2007**, *32*, 138.
- (42) Sosnick, T. R.; Pan, T. *Curr. Opin. Struct. Biol.* **2003**, *13*, 309.
- (43) (a) Das, R.; Kwok, L. W.; Millett, I. S.; Bai, Y.; Mills, T. T.; Jacob, J.; Maskel, G. S.; Seifert, S.; Mochrie, S. G.; Thiyagarajan, P.; Doniach, S.; Pollack, L.; Herschlag, D. *J. Mol. Biol.* **2003**, *332*, 311. (b) Buchmueller, K. L.; Weeks, K. M. *Biochemistry* **2003**, *42*, 13869.
- (44) (a) Adams, A.; Lindahl, T.; Fresco, J. R. *Proc. Natl. Acad. Sci. U.S.A.* **1967**, *57*, 1684. (b) Uhlenbeck, O. C. *RNA* **1995**, *1*, 4. (c) Herschlag, D. *J. Biol. Chem.* **1995**, *270*, 20871.
- (45) Gluick, T. C.; Gerstner, R. B.; Draper, D. E. *J. Mol. Biol.* **1997**, *270*, 451.
- (46) (a) Wu, M.; Tinoco, I., Jr. *Proc. Natl. Acad. Sci. U.S.A.* **1998**, *95*, 11555. (b) Thirumalai, D. *Proc. Natl. Acad. Sci. U.S.A.* **1998**, *95*, 11506.

- (47) Andersen, A. A.; Collins, R. A. *Proc. Natl. Acad. Sci. U.S.A.* **2001**, *98*, 7730.
- (48) Zhang, L.; Xiao, M.; Lu, C.; Zhang, Y. *RNA* **2005**, *11*, 59.
- (49) (a) Pan, J.; Thirumalai, D.; Woodson, S. A. *J. Mol. Biol.* **1997**, *273*, 7. (b) Rook, M. S.; Treiber, D. K.; Williamson, J. R. *J. Mol. Biol.* **1998**, *281*, 609.
- (50) Pan, J.; Woodson, S. A. *J. Mol. Biol.* **1998**, *280*, 597.
- (51) (a) Pan, J.; Deras, M. L.; Woodson, S. A. *J. Mol. Biol.* **2000**, *296*, 133. (b) Russell, R.; Zhuang, X.; Babcock, H. P.; Millett, I. S.; Doniach, S.; Chu, S.; Herschlag, D. *Proc. Natl. Acad. Sci. U.S.A.* **2002**, *99*, 155.
- (52) (a) Banerjee, A. R.; Jaeger, J. A.; Turner, D. H. *Biochemistry* **1993**, *32*, 153. (b) Laggerbauer, B.; Murphy, F. L.; Cech, T. R. *EMBO J.* **1994**, *13*, 2669. (c) Lehnert, V.; Jaeger, L.; Michel, F.; Westhof, E. *Chem. Biol.* **1996**, *3*, 993.
- (53) Pan, J.; Woodson, S. A. *J. Mol. Biol.* **1999**, *294*, 955.

also be explained by the specificity of the folding transitions from U to I_C and I_C to N. In native conditions, thermal fluctuations that result in transient opening of the tertiary structure are expected to produce native-like intermediates that can quickly reform the native structure. By contrast, transient unfolding of the *Tetrahymena* ribozyme, which loses activity above 55 °C,⁵⁴ produces nonnative conformations which cannot easily refold to N.⁵⁵ This may explain why the *Tetrahymena* ribozyme denatures more easily than the *Azoarcus* ribozyme, despite the fact that it is twice the size and contains many more tertiary interactions.

Nucleotide swapping experiments between the *Azoarcus* ribozyme and a less stable relative from *Anabaena* pre-tRNA suggested that the thermostability of the *Azoarcus* ribozyme originates from stronger hydrogen-bonding interactions within the catalytic core.⁵⁶ A similar conclusion was reached from selection of a thermostable variant of the *Tetrahymena* ribozyme^{54,57} and comparisons of the specificity (S) domains of mesophilic and thermophilic RNase P ribozymes.⁵⁸

In another study that compared the stability of the catalytic (C) domains of mesophilic and thermophilic RNase P RNAs, folding of the thermophilic RNA was more cooperative with respect to Mg²⁺ concentration and associated with greater acquisition of structure than folding of its mesophilic relative.⁵⁹ Greater cooperativity in the thermophilic ribozyme was achieved by raising the free energy of an equilibrium folding intermediate, so that the intermediate is no longer populated.⁵⁹ Thus, in both

the *Azoarcus* ribozyme and in the thermophilic RNase P, the stability of the native state is directly related to the cooperativity of the tertiary structure.

Conclusion

Our equilibrium and time-resolved footprinting experiments demonstrate that native tertiary interactions in the *Azoarcus* ribozyme form cooperatively. By stabilizing a native-like intermediate, tertiary interactions also enable the rapid and concerted folding of *Azoarcus* ribozyme. Although RNA folding pathways are often thought to depend on which base pairs form in advance of the tertiary contacts, our results suggest that tertiary interactions between helices make the process of helix assembly more specific and more likely to produce the native architecture. These results strengthen the hypothesis that the early events have significant implications for later events in a folding pathway.^{42,60} They also illustrate the link between thermodynamic cooperativity and the directness of the folding process in RNA.

Acknowledgment. We thank S. Mitra, I. Shcherbakova, J. Schlatterer, and M. Brenowitz for assistance with Kintek experiments. We also thank D. Thirumalai for helpful discussion. This work was supported by a grant from the NIH (GM60809).

Supporting Information Available: Additional Figures (S1–S6) and Tables (S1–S2). This material is available free of charge via the Internet at <http://pubs.acs.org>.

JA076166I

(54) Guo, F.; Cech, T. R. *Nat. Struct. Biol.* **2002**, *9*, 855.

(55) Hopkins, J. F.; Woodson, S. A. *Nucleic Acids Res.* **2005**, *33*, 5763.

(56) Ikawa, Y.; Naito, D.; Shiraishi, H.; Inoue, T. *Nucleic Acids Res.* **2000**, *28*, 3269.

(57) Guo, F.; Gooding, A. R.; Cech, T. R. *RNA* **2006**, *12*, 387.

(58) Baird, N. J.; Srividya, N.; Krasilnikov, A. S.; Mondragon, A.; Sosnick, T. R.; Pan, T. *RNA* **2006**, *12*, 598.

(59) Fang, X. W.; Golden, B. L.; Littrell, K.; Shelton, V.; Thiyagarajan, P.; Pan, T.; Sosnick, T. R. *Proc. Natl. Acad. Sci. U.S.A.* **2001**, *98*, 4355.

(60) Thirumalai, D.; Lee, N.; Woodson, S. A.; Klimov, D. *Annu. Rev. Phys. Chem.* **2001**, *52*, 751.

(61) Adams, P. L.; Stahley, M. R.; Kosek, A. B.; Wang, J.; Strobel, S. A. *Nature* **2004**, *430*, 45.